

A NEW MESH RE-GENERATION METHOD FOR FREE SURFACE FLOW ANALYSIS BASED ON INTERFACE-TRACKING METHOD

Seizo TANAKA¹ and Kazuo KASHIYAMA²

¹Member of JSCE, Research Associate, Dept. of Civil Eng., Chuo University
(1-13-27 Kasuga, Bunkyo-ku, Tokyo 112-8551, Japan)
E-mail: taizo@civil.chuo-u.ac.jp

²Member of JSCE, Professor, Dept. of Civil Eng., Chuo University
(1-13-27 Kasuga, Bunkyo-ku, Tokyo 112-8551, Japan)
E-mail: kaz@civil.chuo-u.ac.jp

This paper presents a new mesh re-generation technique for free surface flow analysis based on the interface-tracking method. The incompressible Navier-Stokes equation based on the arbitrary Lagrangian-Eulerian description is used as the governing equation. The SUPG/PSPG formulation is employed for the finite element discretization. The coupled non-linear finite element equation systems are linearized by the Newton-Raphson method. As numerical examples, the present method is applied to the sloshing problem, the broken-dam problem and the fountain flow problem in a rectangular tank. The efficiency of the present method is shown by these numerical results.

Key Words : *mesh re-generation technique, free surface flow, interface-tracking method, ALE stabilized finite element method*

1. INTRODUCTION

The accurate evaluations of the fluid motion and the force acting to the structure are needed for the planing and the designing of civil structures. Several numerical methods have been presented to analyze the free surface flow problems. Based on the frame of reference used, these approaches can be classified into two approaches: 1) Interface-capturing method using Eulerian stationary mesh and 2) Interface-tracking method using Lagrangian moving mesh. Both approaches have advantages and disadvantages. The interface-capturing method such as the VOF (Volume of fluid) method¹⁾⁻³⁾ or the level-set method⁴⁾ has the robustness in applicability; for example, it can be usefully applied to the problems with complicated free surface motion such as breaking waves. However, as the position of free surface is treated indirectly and determined by solving the advection equation for the interface function, it is necessary to use a fine mesh to obtain the solution with desired accuracy. On the other hand, the interface-tracking method

such as the ALE (arbitrary Lagrangian-Eulerian) method⁵⁾⁻⁹⁾ or the space-time method^{10),11)} is accurate method compared with the interface-capturing method, since the interface is treated as lines or surfaces. However, the method often causes the numerical instability problems when the strong mesh distortion is caused by the complicated behavior of the moving free surface. Thus, a useful mesh re-generation method is required for the cases with complex free-surface shape.

This paper presents a new mesh re-generation method for free surface flow analysis based on the interface tracking approach. A background mesh is introduced in the mesh re-generation algorithm to compute the complex free-surface flow problems. The incompressible Navier-Stokes equation based on the arbitrary Lagrangian-Eulerian description is used as the governing equation. The stabilized finite element method based on the SUPG/PSPG methods¹²⁾ is used. The coupled non-linear finite element equation system is linearized by the Newton-Raphson iterative method and the GMRES technique¹³⁾ based on

the matrix-free method¹⁴⁾ is used to solve the linear equation systems. The stabilized ALE finite element method based on the present mesh re-generation method is applied to the several numerical examples; the sloshing problem, the broken-dam problem and the fountain flow problem in a rectangular tank. The computed results are compared with the experimental and conventional numerical results to show the validity and efficiency of the method.

2. GOVERNING EQUATIONS

The fluid flow can be governed by the unsteady Navier-Stokes equation and the incompressible condition. The momentum and continuity equations in the ALE description can be written as follows:

$$\rho \left(\frac{\partial \mathbf{u}}{\partial t} + \bar{\mathbf{u}} \cdot \nabla \mathbf{u} - \mathbf{f} \right) - \nabla \cdot \sigma(\mathbf{u}, p) = 0 \text{ on } \Omega, (1)$$

$$\nabla \cdot \mathbf{u} = 0 \quad \text{on } \Omega, (2)$$

where $\mathbf{u}(\mathbf{x}, t)$ and $p(\mathbf{x}, t)$ represent the velocity and pressure. The external body force is represented by $\mathbf{f}(\mathbf{x}, t)$, $\bar{\mathbf{u}}$ is the relative velocity including the mesh velocity, Ω is the fluid domain. The density ρ is assumed to be constant. The stress tensor $\sigma(\mathbf{u}, p)$ can be decomposed into its isotropic and deviatoric parts:

$$\sigma(\mathbf{u}, p) = -p \mathbf{I} + 2\mu \varepsilon(\mathbf{u}), (3)$$

$$\varepsilon(\mathbf{u}) = \frac{1}{2} \left(\nabla \mathbf{u} + (\nabla \mathbf{u})^T \right), (4)$$

where μ is the dynamic viscosity. The Dirichlet and Neumann-type boundary conditions are represented as

$$\mathbf{u} = \mathbf{g} \quad \text{on } \Gamma_g, (5)$$

$$\mathbf{n} \cdot \sigma = \mathbf{h} \quad \text{on } \Gamma_h, (6)$$

where Γ_g and Γ_h are complementary subsets of the boundary Γ , \mathbf{n} is the unit outward normal vector.

Boundary conditions imposed on the free surface are kinematic and dynamic ones. The kinematic condition requires that the free surface is a material surface; i.e. the fluid particles which are at some time on the free surface stay always on it. This condition is used to describe the motion of the free surface.

$$\mathbf{u} \cdot \mathbf{n} = \hat{\mathbf{u}} \cdot \mathbf{n} \quad \text{on } \Gamma_{fs}, (7)$$

where $\hat{\mathbf{u}}$ is the mesh velocity. The free surface tension is neglected, and the stress-free condition is imposed as the dynamic condition on the free surface.

3. FINITE ELEMENT FORMULATIONS

(1) Stabilized finite element method

The stabilized finite element formulation based on the SUPG/PSPG method¹²⁾ for Eqs.(1) and (2) can be written as follows:

$$\begin{aligned} & \int_{\Omega} \mathbf{w} \cdot \rho \left(\frac{\partial \mathbf{u}}{\partial t} + \bar{\mathbf{u}} \cdot \nabla \mathbf{u} - \mathbf{f} \right) d\Omega \\ & + \int_{\Omega} \varepsilon(\mathbf{w}) : \sigma(\mathbf{u}, p) d\Omega + \int_{\Omega} q \nabla \cdot \mathbf{u} d\Omega \\ & + \sum_{e=1}^{n_{el}} \int_{\Omega^e} \left\{ \tau_{supg} \bar{\mathbf{u}} \cdot \nabla \mathbf{w} + \tau_{pspg} \frac{1}{\rho} \nabla q \right\} \\ & \cdot \left\{ \rho \left(\frac{\partial \mathbf{u}}{\partial t} + \bar{\mathbf{u}} \cdot \nabla \mathbf{u} - \mathbf{f} \right) - \nabla \cdot \sigma(\mathbf{u}, p) \right\} d\Omega \\ & + \sum_{e=1}^{n_{el}} \int_{\Omega^e} \tau_{cont} \nabla \cdot \mathbf{w} \rho \nabla \cdot \mathbf{u} d\Omega \\ & = \int_{\Gamma_h} \mathbf{w} \cdot \mathbf{h} d\Gamma, \end{aligned} (8)$$

where \mathbf{w} and q are weighting functions for the momentum and continuity equations, respectively. τ_{supg} , τ_{pspg} and τ_{cont} are stabilization parameters which are defined as follows¹¹⁾:

$$\tau_{supg} = \left[\left(\frac{2}{\Delta t} \right)^2 + \left(\frac{2\|\mathbf{u}\|}{h_e} \right)^2 + \left(\frac{4\nu}{h_e^2} \right)^2 \right]^{-\frac{1}{2}}, (9)$$

$$\tau_{pspg} = \tau_{supg}, (10)$$

$$\tau_{cont} = \frac{h_e}{2} \|\mathbf{u}\| \xi(Re_e), (11)$$

where, Δt is the time increment, h_e is the element length and Re_e is the element level Reynolds number.

Using the P1P1 (continuous linear interpolation both for velocity and pressure) element for the spatial discretization of Eq.(8), the following finite element equations can be obtained:

$$\begin{aligned} & (\mathbf{M} + \mathbf{M}_{\delta}) \frac{\partial \mathbf{u}}{\partial t} + (\mathbf{A} + \mathbf{A}_{\delta}) \mathbf{u} \\ & + \mathbf{D} \mathbf{u} - (\mathbf{G} - \mathbf{G}_{\delta}) p = \mathbf{F} + \mathbf{F}_{\delta}, \end{aligned} (12)$$

$$\mathbf{G}^T \mathbf{u} + \mathbf{M}_{\varepsilon} \frac{\partial \mathbf{u}}{\partial t} + \mathbf{A}_{\varepsilon} \mathbf{u} + \mathbf{G}_{\varepsilon} p = \mathbf{F}_{\varepsilon}, (13)$$

where, \mathbf{M} , \mathbf{A} , \mathbf{D} , \mathbf{G} and \mathbf{F} are the matrices for the time-dependent, convection, viscous, pressure gradient, and external force terms, respectively. The subscripts δ and ε indicate the contribution from SUPG and PSPG, respectively.

The full implicit scheme is used for the temporal discretization of Eqs.(12), (13). The time derivative term can be discretized as:

$$\frac{\partial \mathbf{u}}{\partial t} = \frac{\mathbf{u}_{n+1} - \mathbf{u}_n}{\Delta t}, (14)$$

where n and $n + 1$ denote time levels n and $n + 1$. And the velocity \mathbf{u} and pressure p are discretized as follows:

$$\mathbf{u} = \alpha \mathbf{u}_{n+1} + (1 - \alpha) \mathbf{u}_n, \quad (15)$$

$$p = p_{n+1}, \quad (16)$$

where α is the parameter which controls the temporal stability and accuracy. (Nomarily α is assume to be 0.5.)

(2) Iterative method

From the above discretization in space and time, a non-linear equation system can be obtained as:

$$\mathbf{R}(\mathbf{d}_{n+1}) = 0, \quad (17)$$

where, \mathbf{d}_{n+1} is the nodal values of the unknowns (\mathbf{u} and p) corresponding to the time step level $n + 1$. The Eq.(17) is solved by the Newton-Raphson iterations:

$$\mathbf{J}_{n+1}^k(\Delta \mathbf{d}_{n+1}^k) = -\mathbf{R}(\mathbf{d}_{n+1}^k) \quad (18)$$

where \mathbf{d}_{n+1}^k is the k th iteration value of \mathbf{d}_{n+1} , \mathbf{J}_{n+1}^k is the approximate derivative of \mathbf{R} with respect to \mathbf{d}_{n+1} , evaluated at \mathbf{d}_{n+1}^k , and $\Delta \mathbf{d}_{n+1}^k$ is the correction computed for \mathbf{d}_{n+1}^k . The GMRES method¹³⁾ based on the matrix-free method¹⁴⁾ is employed to solve Eq.(18).

(3) Mesh update method

In the interface tracking method, the finite element mesh over the fluid domain must be deformed in accordance with the free-surface motion governed by kinematic free-surface condition (7). In order to express the arbitrary free surface shapes, the mesh velocity on the free surface is defined as follows:

$$\hat{\mathbf{u}} = (\mathbf{u} \cdot \mathbf{n}) \mathbf{n}, \quad (19)$$

The displacements of internal node \mathbf{v} can be governed by the linear elasticity equation:

$$\nabla \cdot \sigma_m(\mathbf{v}) = 0, \quad \text{on } \Omega, \quad (20)$$

with the constitutive equation defined as:

$$\sigma_m(\mathbf{v}) = \lambda_m (\text{tr } \varepsilon_m(\mathbf{v})) \mathbf{I} + 2\mu_m \varepsilon_m(\mathbf{v}), \quad (21)$$

$$\varepsilon_m(\mathbf{v}) = \frac{1}{2} (\nabla \mathbf{v} + (\nabla \mathbf{v})^T), \quad (22)$$

The following boundary conditions are employed to solve for the displacement field;

$$\mathbf{v} = \mathbf{g}_m \quad \text{on } \Gamma_{g_m}, \quad (23)$$

$$\mathbf{n} \cdot \sigma_m = \mathbf{h}_m \quad \text{on } \Gamma_{h_m}. \quad (24)$$

The standard Galerkin finite element method is applied to the spatial discretization of Eq.(20) and the Element-by-Element SCG method is

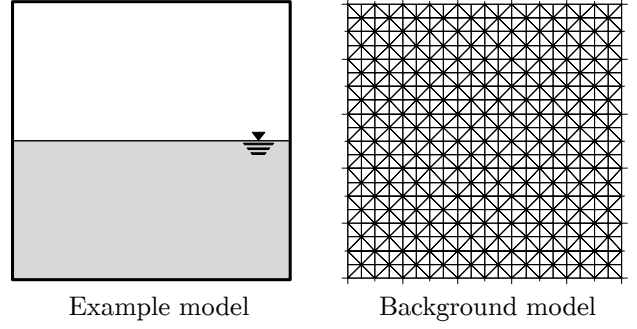


Fig.1 Example model and background mesh

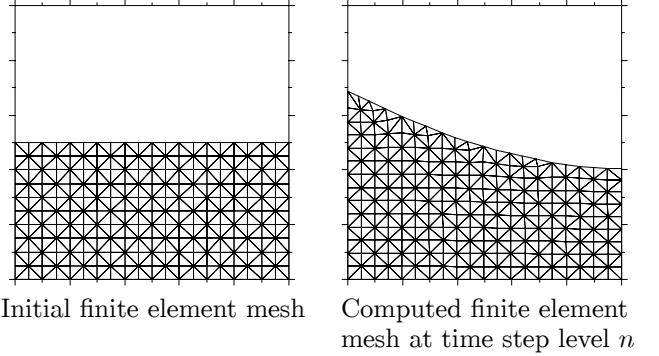


Fig.2 Initial finite element mesh and computed finite element mesh at time step level n

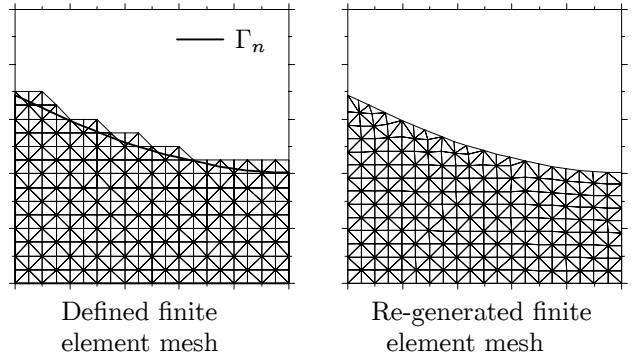


Fig.3 Defined and re-generated finite element mesh

employed to solve the discretized linear elasticity equation. The mesh update is carried out by the relocation of nodes as follows:

$$\mathbf{x}_{n+1} = \mathbf{x}_n + \mathbf{v}. \quad (25)$$

4. MESH RE-GENERATION METHOD USING BACKGROUND MESH

The mesh re-generation algorithm using a background mesh is introduced to compute the complex free surface flow problems. We use an example model shown in Fig.1(left) to explain the mesh re-generation algorithm for free surface flow problem. Fig.1(right) shows the background mesh for this model. The computation was

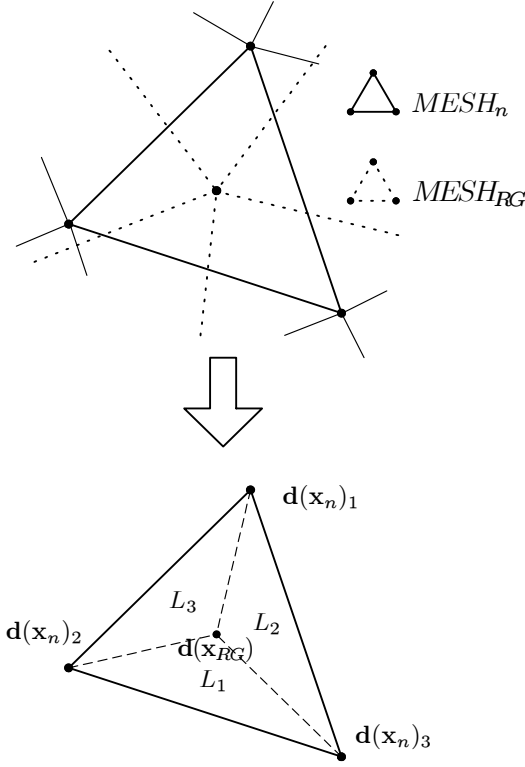


Fig.4 Model of the correction of physical values

started with the initial mesh shown in **Fig.2**(left), and **Fig.2**(right) shows the computed finite element mesh at time step level n . We generate a new finite element mesh for the domain surrounded by the boundary of the computed domain Γ_n . The following procedures are applied at every time step level to consider the shape of free surface.

(1) Consideration of the free surface

- (a) Defining Step : The finite element mesh is defined to contain the boundary of fluid domain at time step level n from the background mesh shown in **Fig.1**(right). **Fig.3**(left) shows the defined finite element mesh. In this figure, the bold line denotes the boundary of the domain at time step level n .
- (b) Fitting Step : The nodes on the boundary of the defined finite element mesh (the nodes are located outside the free surface in **Fig.3**(left)) are fitted to the free surface at time step level n . The position of interior nodes are determined by solving the linear elasticity equation (20). **Fig.3**(right) shows the re-generated finite element mesh ($MESH_{RG}$) used in the computation.

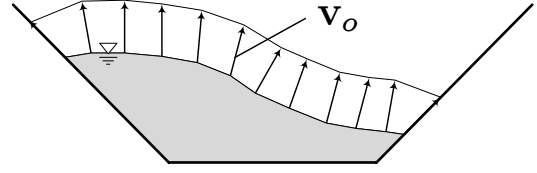


Fig.5 Volume correction

(2) Correction of the physical value

The nodal values for the velocity and pressure in the re-generated finite element mesh ($MESH_{RG}$) must be corrected by using the computed nodal values in the mesh at time step level n ($MESH_n$). In this correction, the cubic interpolation based on CIVA scheme¹⁵⁾ is used as shown in **Fig.4**. The nodal values $\mathbf{d}(\mathbf{x}_{RG})$ are interpolated in the following form via the area coordinates (L_1, L_2, L_3):

$$\mathbf{d}(\mathbf{x}_{RG}) = \left[\sum_{i=1}^3 \mathbf{a}_i L_i + c \sum_{j,k=1}^3 \mathbf{b}_{jk} [L_j^2 L_k + \frac{1}{2} L_1 L_2 L_3] \right] \Big|_{\mathbf{x}_n}, \quad (26)$$

$$\mathbf{a}_i = \mathbf{d}_i, \quad (27)$$

$$\mathbf{b}_{jk} = \mathbf{d}_j - \mathbf{d}_k + (\mathbf{x}_k - \mathbf{x}_j) \cdot \nabla \mathbf{d}_j, \quad (28)$$

where c is the parameter for the interpolation, and served as the cubic interpolation in the case of $c = 1$ and the linear interpolation in the case of $c = 0$. The spatial derivatives of the nodal values $\nabla \mathbf{d}$ are recovered using the least-squares approach.

From the above procedures, a new finite element mesh with the nodal values is re-generated.

5. VOLUME CORRECTION METHOD

In order to satisfy the mass conservation of fluid, the volume correction method is introduced to offset the error of volume at every time step level. The error of volume is mainly caused by the projection error occurred at the fitting step in the mesh re-generation method. The offset of the error of volume is achieved by the node relocation on the free surface as:

$$\mathbf{v}_o = \gamma \mathbf{n}, \quad (29)$$

where \mathbf{v}_o denotes the node displacement on the free surface, γ is the offset parameter which can be defined as:

$$\gamma = \frac{V_T - V_n}{\int_{\Gamma_{fs}} \mathbf{n} \cdot \mathbf{n} d\Gamma}, \quad (30)$$

where V_T is the target volume of the fluid and V_n is the computed volume at the n th time step level

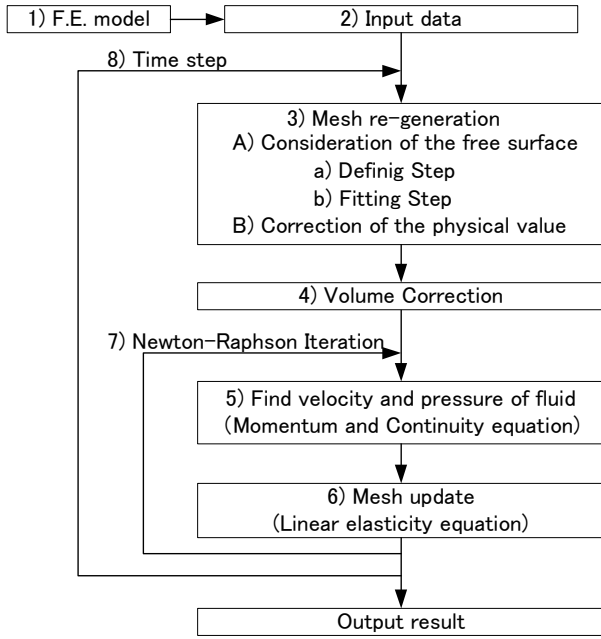


Fig.6 Flow chart of the computation

(see **Fig.5**). The position of interior nodes are determined by solving the linear elasticity equation (20).

6. ALGORITHM OF THE COMPUTATION

The flow chart of the computation is shown in **Fig.6**. The algorithm can be written as follows:

- 1) A background mesh and the initial position of the free surface are set.
- 2) The input data for the finite element mesh, the initial condition and the boundary condition are given.
- 3) The finite element mesh is re-generated using the position of the free surface, and the nodal values are corrected.
- 4) The node on the free surface is relocated to offset the error of volume of fluid.
- 5) Eq.(18) is solved by the GMRES method to find the approximate solution for the velocity \mathbf{u} and pressure p .
- 6) The linear elasticity equation (20) is solved by the E-By-E SCG method for mesh update.
- 7) The Newton-Raphson iteration loop 5)~6) is repeated until the convergence is realized.
- 8) The time step loop 3)~7) is repeated until the final time level.

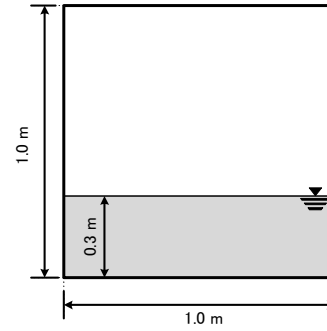


Fig.7 Numerical model of rectangular tank

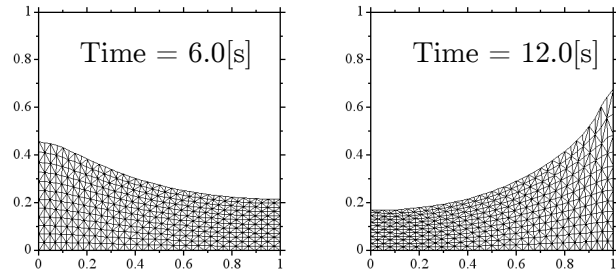


Fig.8 Computed free surface shapes without mesh re-generation

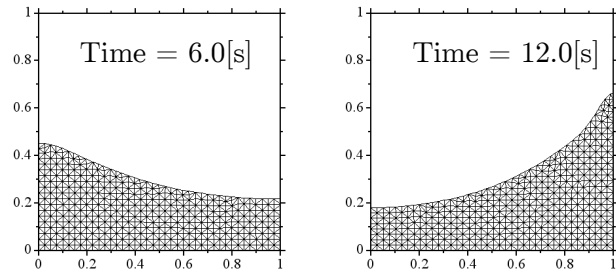


Fig.9 Computed free surface shapes with mesh re-generation

7. NUMERICAL EXAMPLES

The present method is applied to several numerical examples; the sloshing problem, the broken-dam problem, and the fountain flow problem in a rectangular tank.

(1) Sloshing problem in a rectangular tank

In order to show the validity of the present method, the method is applied to the two dimensional sloshing problem in a rectangular tank. **Fig.7** shows the numerical model and the whole domain is discretized by an uniform finite element mesh with 40×40 elements ($x \times y$ direction) as the background mesh. The density and kinematic viscosity of water are assumed to be 1.0×10^3 [kg/m^3] and 1.0×10^{-6} [m^2/s], respectively. The free-slip boundary condition is applied to the walls. The sloshing wave is generated by applying

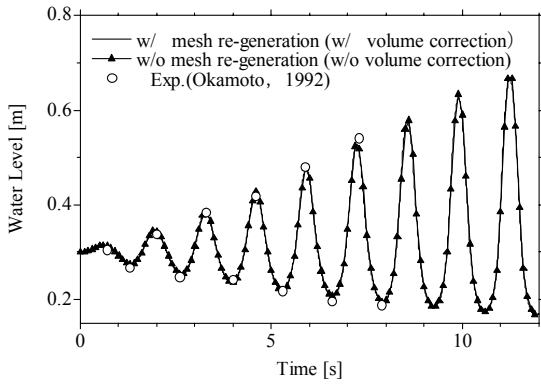


Fig.10 Time history of water level at the left-side wall

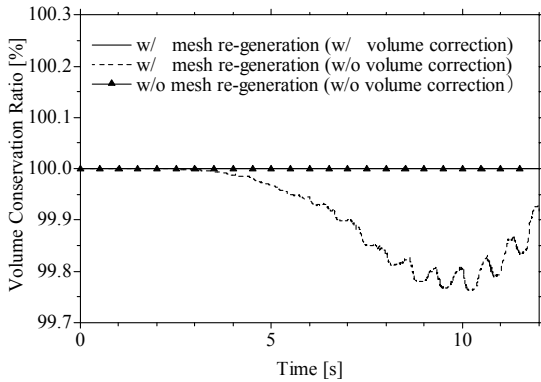


Fig.11 Time history of volume conservation ratio

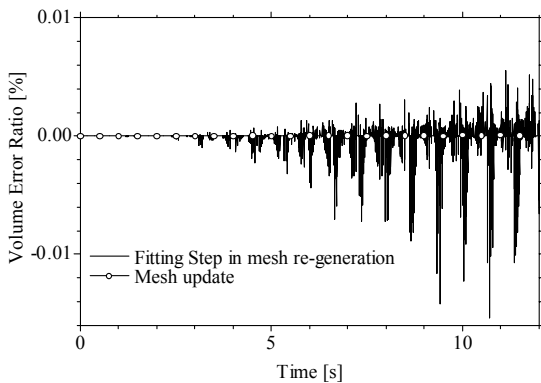


Fig.12 Volume error ration at each time step

a horizontal body force to the tank as:

$$f_x = A\omega^2 \sin \omega t, \quad (31)$$

where A is the amplitude and ω is the frequency ($A = 0.0093$ [m], $\omega = 4.761$ [rad/s]). The time increment Δt is assumed to be 1.0×10^{-3} [s]. In order to check the validity of the present mesh re-generation method, the computed results are compared with the results obtained by the method without mesh re-generation. In the case without mesh re-generation, the nodes on the free surface are allowed to move in a vertical direction only, and the volume correction method is omitted. **Fig.8** shows the computed

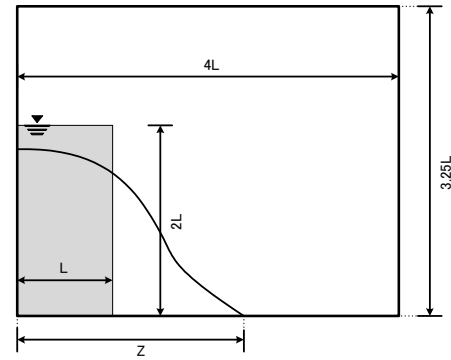


Fig.13 Numerical model

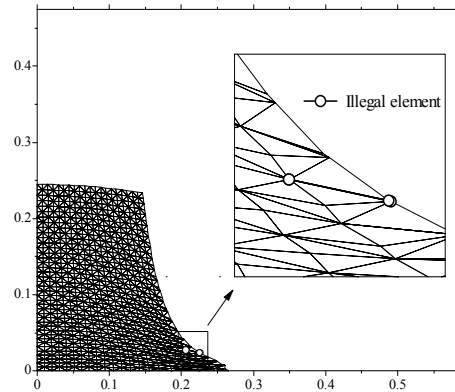


Fig.14 Computed fluid domain without mesh re-generation method

free surface shape without mesh re-generation, and **Fig.9** shows the computed free surface shape with mesh re-generation at each time step level. From these figures, the computed results by the present method are in good agreement with the results without the mesh re-generation method. **Fig.10** shows the time history of the water level at the left-side wall, the computed results with the mesh re-generation method is also in good agreement with the computed result without the mesh re-generation method and the experimental result by Okamoto⁵⁾. From this figure, it can be recognized that the mesh re-generation method is not needed in this example because the shape of free surface is not so complicated.

Fig.11 shows the comparison of the time history of volume conservation ratio. From this figure, the conservation of volume is satisfied in the case without the mesh re-generation and volume correction methods, and the result with the mesh re-generation and volume correction methods. On the other hand, the case with mesh re-generation and without volume correction can not satisfy the conservation of volume. From this figure, it can be concluded that the volume correction method is needed if the mesh re-generation method is employed. In order to investigate the

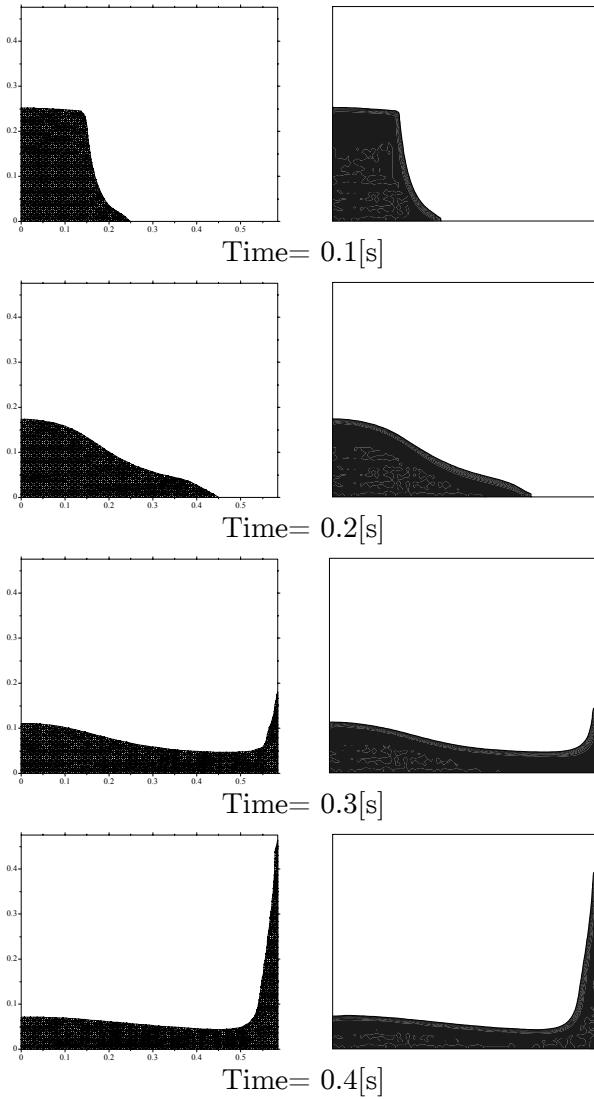


Fig.15 Computed free surface shapes (left:present method, right:CIVA/VOF method)

cause of the volume error, **Fig.12** shows the volume error ratio occurred in the fitting step of mesh re-generation (shown in the flow chart 3) A) b)) and in the mesh update (shown in the flow chart 6)) at each time step. From this figure, the volume error is not found in the mesh update step but in the fitting step. The accumulation of this error at each time step leads to the volume error as shown in **Fig.11**.

(2) Broken-dam problem

The present method is applied to the broken-dam problem. The rectangular computational domain is surrounded by solid walls, as shown in **Fig.13**. The initial water column is assumed to be $L=0.146$ [m] in width and $2L$ in height. The computational domain is subdivided into a uniform mesh of 80×65 elements ($x \times y$ direction) as the background mesh. The time increment is as-

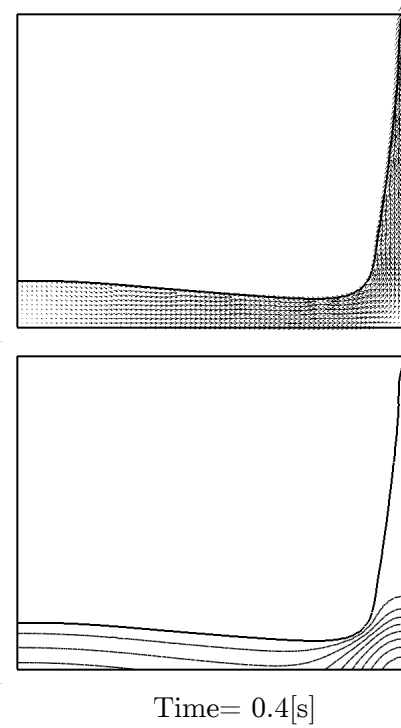


Fig.16 Velocity vector and pressure contour

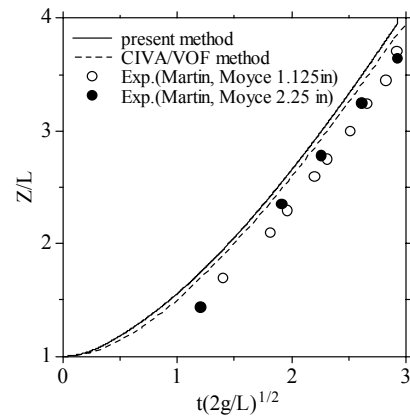


Fig.17 Time history of the water front location

sumed to be 2.0×10^{-4} [s]. **Fig.14** shows the finite element mesh without the mesh re-generation method. The computation is stopped by the occurrence of the illegal elements at the stage shown in **Fig.14**. **Fig.15** shows the computed result with the mesh re-generation method. From this, it can be seen that the mesh re-generation is needed for the simulation of free surface flows with the large deformation of fluid. **Fig.15** also shows the computed results by the CIVA/VOF method³⁾, which is one of the interface-capturing methods. From this figure, the computed free surface shape by the present method is in good agreement with the computed results by the CIVA/VOF method. The velocity vector and pressure contours obtained by the present method are shown in **Fig.16**. As can be seen from these

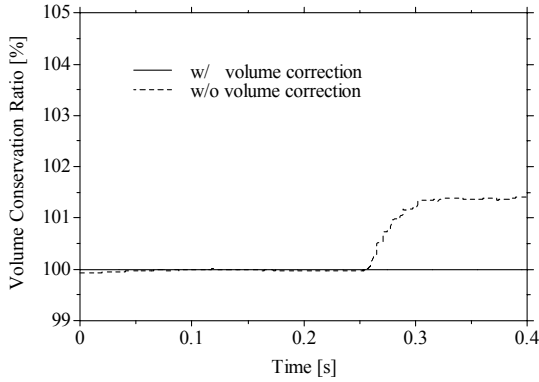


Fig.18 Time history of the volume conservation ratio

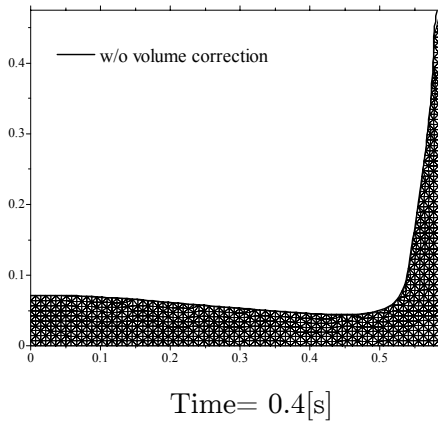


Fig.19 Influence of the volume correction

figures, the stable computation is realized by the introduction of the mesh re-generation method. **Fig.17** shows the comparison of the time histories of the water front location. The solid line shows the present numerical result and the dotted line shows the result of CIVA/VOF method, and the solid circles denote the experimental data¹⁶⁾. From this figure, the computational result by the present method is in good agreement with the experimental data and the result by the CIVA/VOF method. The time history of the volume conservation ratio is shown in **Fig.18**. From this, the case without the volume correction method suffers from the increase of the volume. On the other hand, the case with volume correction satisfies the volume conservation. **Fig.19** shows the effect of volume correction to the free surface shape. From this figure, the volume correction method does not give a bad effect to the representation of free surface shape.

(3) Fountain flow problem

Finally, the present method is applied to the fountain flow problem as an application example. **Fig.20** shows the computational model. The inviscid fluid is assumed in this example. The grav-

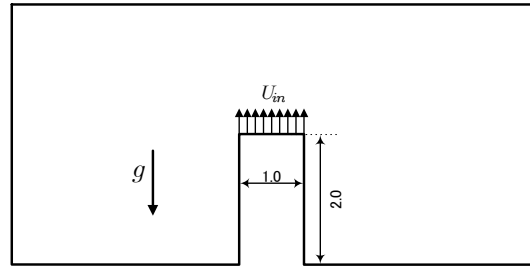


Fig.20 Numerical model

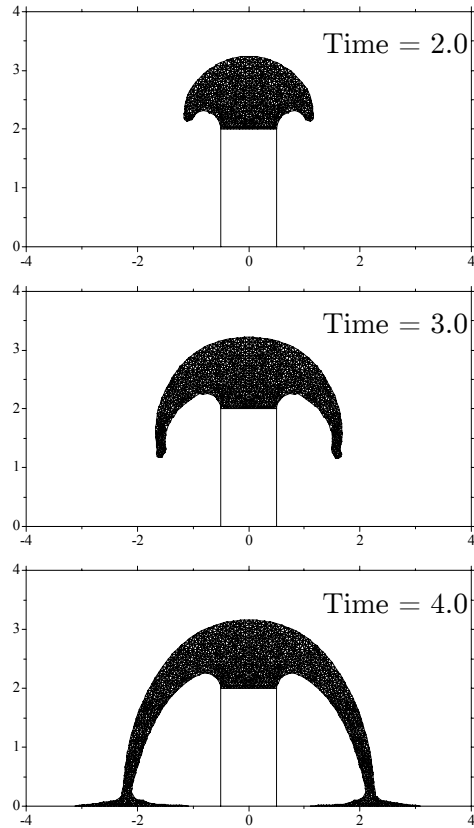


Fig.21 Computed fluid domain

itational acceleration, and the vertical inflow velocity are assumed to be $g = 1.0$, and $U_{in} = 1.0$, respectively. The density and kinematic viscosity of the fluid are assumed to be 1.0 and 0, respectively. The evolution of the fluid domain and its mesh is shown in **Fig.21**. It can be seen from this figure that the computation is carried out stably for the free surface flow with the complicated free surface shapes.

8. CONCLUSIONS

A new mesh re-generation method using a background mesh has been presented for free surface flow analysis. The stabilized ALE finite element based on the SUPG/PSPG method has been applied to several numerical examples; the sloshing

problem, the broken-dam problem and the fountain flow problem in a rectangular tank. The following conclusions are obtained:

- The computed results obtained by the present method are in good agreement with the experimental results and the numerical results obtained by the conventional method based on the interface-capturing method.
- By introduction of the present mesh regeneration method, the applicability and the robustness of the method is improved.
- The present method is useful to evaluate the fluid forces since the boundary is expressed directly compared with the interface capturing method. This point has advantage for the planning and designing of structure.

From the results obtained in this paper, it can be concluded that the present method is a useful method for the complicated free surface flow problems. For the future works, we plan to investigate the projection error occurred at the fitting step, and to apply the present method for the three dimensional analysis.

ACKNOWLEDGEMENT: This research was supported by the grant-in-aid for scientific research of the Japan society for the promotion of science, No.15560409.

REFERENCES

- 1) Hirt, C.W., Nichols, B.D.: Volume of fluid (VOF) method for the dynamics of free boundaries, *Journal of Computational Physics*, Vol.39, pp.201-225, 1981.
- 2) Nakayama, T., Shibata, M.: A finite element technique combined with gas-liquid two-phase flow calculation for unsteady free surface flow problem, *Computational Mechanics*, Vol.22, pp.194-202, 1988.
- 3) Sakuraba, M., Hirosaki, S., Kashiyama, K.: Development of accurate interface-capturing method for free surface flow analysis based on CIVA/VOF method, *Journal of Applied Mechanics*, JSCE, Vol.6, pp.215-222, 2003.(in Japanese)
- 4) Sussman, M., Smereka, P., Osher, S.: A level set approach for computing solution for incompressible two-phase flow, *Journal of Computational Physics*, Vol.114, pp.146-202, 1994.
- 5) Okamoto, T., Kawahara, M.: Tow-dimensional sloshing analysis by Arbitrary Lagrangian-Eulerian finite element methods, *Proceeding of JSCE*, No.441/I-18, pp.39-48, 1992.
- 6) Nomura, T.: ALE finite element computations of fluid-structure interaction problems, *Computer Methods in Applied Mechanics and Engineering*, Vol.112, pp.291-308, 1994.
- 7) Sakuraba, M., Tanaka, S., Kashiyama, K.: ALE parallel finite element analysis of non-linear free surface flows using PC cluster, *Journal of Applied Mechanics*, JSCE, Vol.4, pp.113-120, 2001.(in Japanese)
- 8) Kashiyama, K., Tanaka, S., Sakuraba, M.: PC cluster finite element analysis of sloshing problem by earthquake using different network environments, *Communication in Numerical Methods in Engineering*, Vol.18, pp.681-690, 2002.
- 9) Tanaka, S., Kashiyama, K.: ALE Stabilized finite element method for free surface flows with an arbitrary shape of wall and an outflow boundary, *Journal of Applied Mechanics*, JSCE, Vol.6, pp.223-230, 2003. (in Japanese)
- 10) Behr, M., Tezduyar, T.E.: Finite element solution strategies for large-scale flow simulations, *Computer Methods in Applied Mechanics and Engineering*, Vol.112, pp.3-24, 1994.
- 11) Güler, I., Behr, M. and Tezduyar, T.E.: Parallel finite element computation of free-surface flows, *Computational Mechanics*, Vol.23, pp.117-123, 1999.
- 12) Tezduyar, T.E.: Stabilized finite element formulations for incompressible flow computations, *Advanced in Applied Mechanics*, Vol.28, pp.1-44, 1991.
- 13) Saad, Y., Schultz, M.: GMRES: A generalized minimal residual algorithm for solving nonsymmetric linear systems, *SIAM J. Scientific and Statistical Computing*, Vol.7, pp.856-869, 1986.
- 14) Johan, Z., Hughes, T.J.R., Mathur, K.K. and Johansson, S.L.: A data parallel finite element method for computational fluid dynamics on the Connection Machine system, *Computer Methods in Applied Mechanics and Engineering*, Vol.99, pp.113-134, 1992.
- 15) Tanaka, N.: 'The CIVA method for mesh-free approaches': improvement of the CIP method for n-simplex, *Computational Fluid Dynamics Journal*, Vol.8, no.1, pp.121-127, 1999.
- 16) Martin, J.C. and Moyce, W.J.: An experimental study of the collapse of liquid columns on a rigid horizontal plane, *Phil. Trans. Roy. Soc. London A*, Vol.244, pp.312-324, 1952.

(Received February 9, 2006)